JTTEE5 14:354-361
DOI: 10:1361/105996305X59422
1059-9630/$19.00 © ASM International

Peer Reviewed

Photographing Impact of Molten Molybdenum Particles in a Plasma Spray

N.Z. Mehdizadeh, M. Lamontagne, C. Moreau, S. Chandra, and J. Mostaghimi

(Submitted June 2, 2004; in revised form September 28, 2004)

Plasma-sprayed molten molybdenum particles (~40 μm in diameter) were photographed impinging at high velocity (~140 m/s) on a glass substrate at room temperature. An optical sensor detected thermal radiation emitted by a droplet as it approached the substrate and activated a time delay unit. After a selected time interval, an Nd:YAG laser was triggered, emitting a 5 ns pulse that provided illumination for a charge-coupled device (CCD) camera to photograph the impacting droplet through a long-range microscope. By varying the delay before pulsing the laser, different stages of droplet deformation were recorded. Impacting droplets spread into a thin circular film that ruptured and broke into small fragments. An optical detector recording thermal radiation from the impacting droplet gave a signal that increased as the droplet spread out, reached a maximum when the liquid film began to rupture, and decreased as portions of the droplet recoiled because of surface tension and then flew out of view of the photodetector.

Keywords droplet, particle impact, plasma spray, splashing, splat

1. Introduction

Plasma spray coatings are applied by feeding metal or ceramic powders into a high-temperature plasma jet directed onto a surface. Powder particles melt when introduced into the hot gas, flatten upon impact with the solid substrate, and freeze rapidly to form a dense deposit. Coating properties such as adhesion strength and porosity depend on the dynamics of molten droplet impact. If droplets splash during impact, producing solidified splats that are fragmented and irregular in shape, coatings are porous and do not adhere well (Ref 1, 2). Coating material is wasted by droplet splashing because secondary droplets bounce off the surface instead of adhering. Ideally there should be no splashing during droplet impact, so that splats are disk-shaped with a smooth, circular periphery.

Experiments have shown that splat shape is affected by many process variables such as substrate temperature, wettability, and roughness; droplet temperature and velocity; and volatile compounds adsorbed on the surface (Ref 3-8). There has been much conjecture as to the mechanism of splashing, with several explanations offered, including fluid instabilities, flow obstructions caused by solidification around the edges of spreading droplets, and escape of adsorbed vapor as the surface under impacting droplets is heated. Most of these hypotheses are based on microscopic examinations of splats left after droplet impact. The small size (typically ~30-50 μm diameter) and high-impact velocity (>100 m/s) of droplets in a plasma spray have made it difficult to observe their impact directly.

N.Z. Mehdizadeh and **M. Lamontagne,** National Research Council of Canada, Industrial Materials Institute, Boucherville, Québec J4B 6Y4, Canada; and **C. Moreau, S. Chandra,** and **J. Mostaghimi,** Centre for Advanced Coating Technologies, University of Toronto, Toronto, Ontario M5S 3G8, Canada. Contact e-mail: Christian.Moreau@cnrc-nrc.gc.ca.

Computer simulations (Ref 9) of droplet impact have offered some insight into what occurs when a thermal spray particle lands on a smooth, unheated surface. Numerical models predict that as the droplet spreads, its periphery solidifies, obstructing flow of liquid and triggering splashing. Lack of any direct observations of particle impact in thermal sprays has, however, meant that there is no way to establish the accuracy of these simulations.

Indirect observation of droplet dynamics were made (Ref 10, 11) using a fast-response optical sensor to measure the intensity of radiation emitted by droplets in plasma sprays as they landed on a glass surface. The results were difficult to interpret directly because thermal radiation emitted depends on both the area of the emitting surface and its temperature. These two effects are hard to separate because the surface areas of droplets change very rapidly as they spread, recoil, and break up, while at the same time droplets cool at rates of 10^6-10^8 K/s. An independent measurement of droplet surface area in contact with the substrate was obtained (Ref 12, 13) during impact of molybdenum droplets on a glass slide by shining a laser beam through the substrate and using an optical detector to measure the fraction of light blocked by spreading droplets. This method gave the area of each droplet but no information on droplet splashing and breakup.

The main objective of this work was to develop a technique to photograph the impact of plasma-sprayed molten molybdenum droplets on a glass substrate. An optical sensor, similar to that described in earlier publications (Ref 12, 13), was used to detect a droplet as it approached the surface. A time delay unit was used to trigger a camera and a laser that provided illumination to photograph the droplet as it collided with the surface. This paper describes the experimental technique and presents some of the images recorded.

2. Experimental Method

Figure 1 shows a schematic of the experimental apparatus used to deposit molten metal droplets on a glass surface and pho-

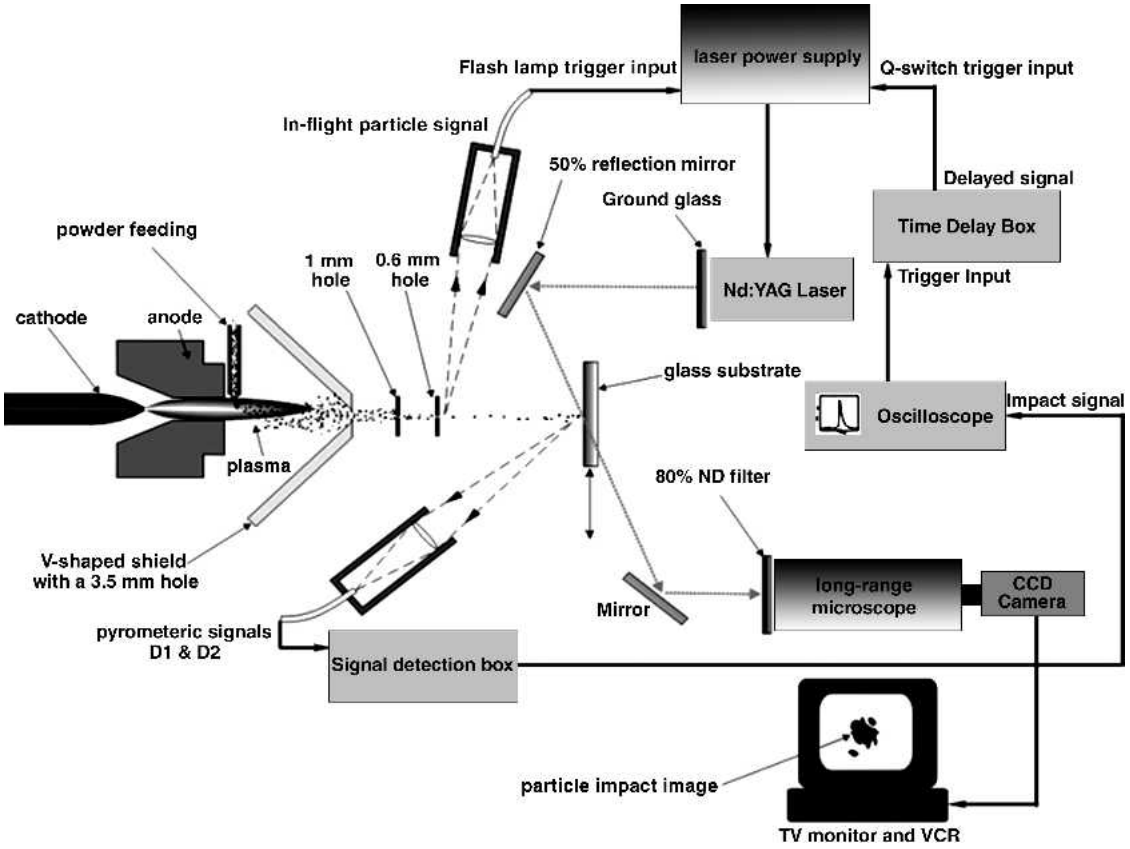

Fig. 1 Schematic of the experimental setup

tograph their impact. Plasma spraying was carried out with a Plasmadyne SG100 torch (Praxair Surface Technologies, Indianapolis, IN). The plasma torch was operated with a gas mixture of 50 L/min argon and 24.6 L/min helium flowing through it. To generate plasma, an electric arc was struck between two electrodes in the gun using an arc current of 700 A. Dense, spherical molybdenum powder particles (SD152, Osram Sylvania Chemical & Metallurgical Products, Towanda, PA) sieved to a narrow size range of 32-45 μm, were fed into the plasma at a very low feed rate of a few g/min.

The plasma gun was mounted on a robot arm and swept rapidly past the substrate (robot speed 15 mm/s) to prevent too many particles from landing on its surface. The spray of droplets passed through a succession of holes in three shielding plates to ensure that only a few droplets impinged on the test surface, which was placed about 70 mm from the plasma torch exit. The first hole, 3.5 mm in diameter, was in a V-shape metal shield that helped protect the surface from the heat of the plasma gun. The second hole, placed 29 mm from the substrate, was 1 mm in diameter; and the third, located 26 mm from the substrate, was 0.6 mm in diameter. The holes were aligned such that only droplets with a horizontal trajectory passed through all three. This helped ensure that droplets that landed on the test surface had a relatively narrow velocity distribution. In total, 95 trials were carried out, of which only 54 resulted in a particle being detected on the surface. The test surface was a precleaned glass slide (Fisher Scientific, Pittsburgh, PA) mounted on a stepper motor-driven stage that was moved to expose a fresh area each time a droplet landed on it.

As a droplet approached within 1 mm of the test surface it passed through the view field of an optical sensor head consisting of a custom-made lens (Ref 14) that focused collected radiation onto the tip of an 800 μm diameter optical fiber with a magnification of 0.46×. The end of the optical fiber was covered with an opaque mask that had three slits etched in it as shown in Fig. 2(a), which allowed measurement of particle thermal radiation at three different positions along the particle trajectory with the same sensors. Two of the slits were narrow, 30 μm in width with centers 60 μm apart, and the last was 150 μm wide. As a result, the sensor picked up radiation along three parallel planes just above the test surface, inclined at an angle of 26° to it (Fig. 2b). When molten molybdenum droplets landed on the glass surface within the 700 × 700 μm area viewed by the optical sensor, they passed through each region in succession before impact.

Thermal radiation collected by the lens was transmitted through an 8 m long optical fiber to a detection unit containing optical filters and two photodetectors. The beam was divided into two equal parts with a beam splitter. Each half was transmitted through a band pass filter, one centered at 790 nm and the other at 1000 nm, and focused on an avalanche silicon photodetector. These wavelengths were chosen to avoid the main emission lines of argon plasma, which could otherwise bias particle thermal emission measurements. Particle temperatures were measured from the ratio of these two signals, using principles of

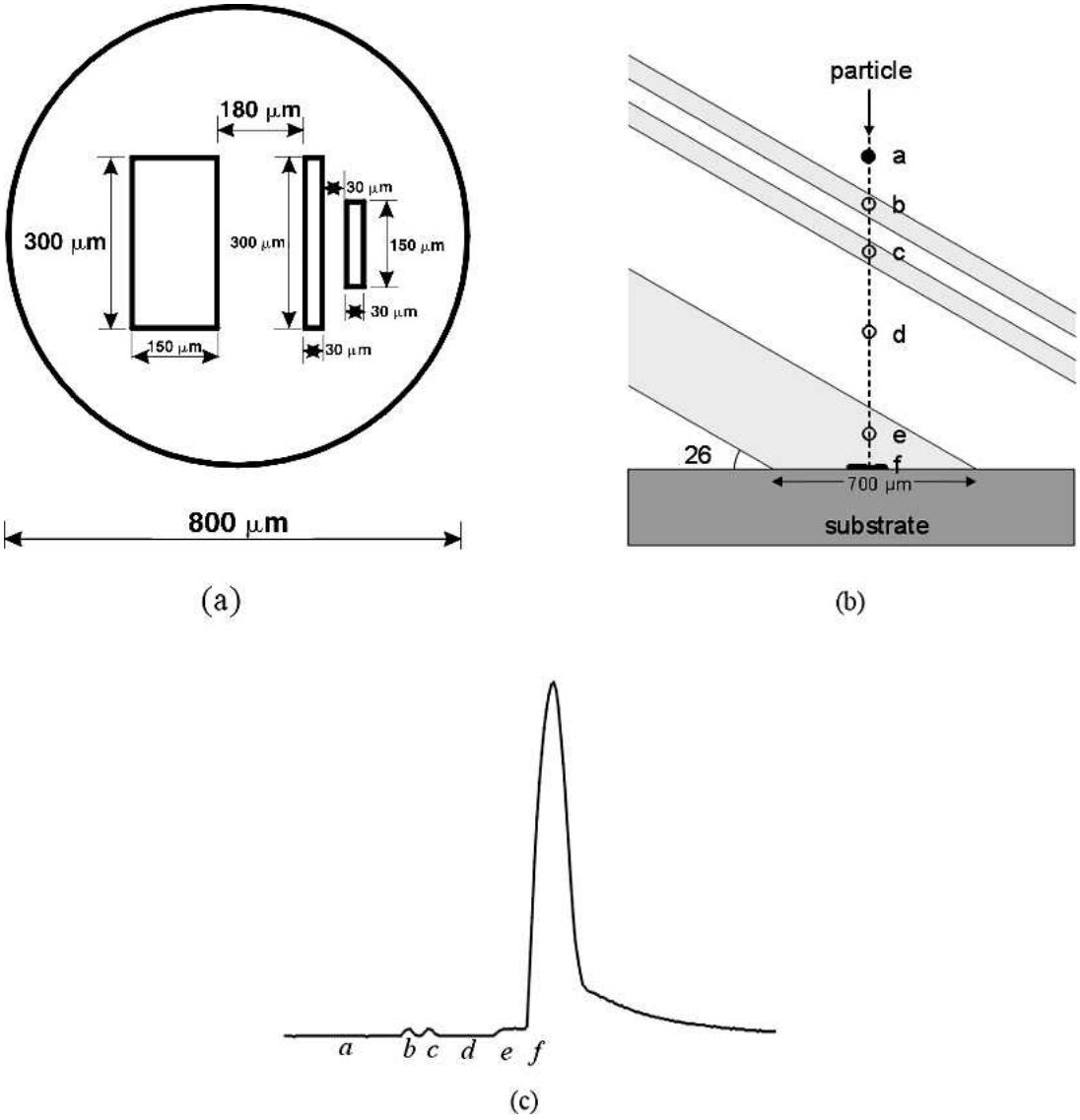

Fig. 2 (a) Schematic of the three-slit mask, (b) optical detector field of view, and (c) thermal emission signal collected by the three-slit mask

two-color pyrometry (Ref 10), assuming that particles were gray bodies. Droplet diameters were estimated by assuming that they were spherical prior to impact, disk-shaped after impact, and had an emissivity of 0.6. The emissivity value was selected by matching the mean particle size measured from the photodetector signal with that obtained from microscopic examination of the powder. Signals were recorded with a 12-bit (5 MHz bandwidth) digital oscilloscope. Diameter measurements from pyrometric signals were estimated to be accurate within ±15%.

A typical signal from an impacting droplet looks like the one shown in Fig. 2(c). Labels *a-f* on the curve correspond to droplet positions marked in Fig. 2(b). The two small peaks labeled *b* and *c* were produced by emission from droplets crossing the field of view of the first two slits. Droplet velocity was calculated by measuring the time interval between the two peaks. At *e* the droplet entered the detection volume of the third slit. Then, as the droplet hit the surface and began to spread out, the area of the emitting surface increased very rapidly, producing a sudden rise in the optical signal at *f*. The signal reached a maximum and then decreased. The decrease could be the result of two factors: the droplet cooled when it spread on the surface; or its surface area decreased as it fragmented, and portions recoiled or flew out of the sensor detection area. Without photographs of droplets during impact it is difficult to differentiate between these two possibilities.

Photographs were taken with a charge-coupled device (CCD) video camera (model WV-CL 324, Panasonic, Montreal, QC) coupled with a long-range microscope (Questar QM100, Company Seven, Astro-optics Division, Montpelier, MD). The camera had a field of view 1.8 mm wide, which was more than twice that of the optical sensor (0.7 mm). The camera operated continuously at a rate of 30 frames/s, so each frame had an exposure of 33 ms. To eliminate blurred images of fast-moving droplets, laser pulses with 20 mJ power and 5 ± 2 ns duration emitted by an Nd:YAG laser (MINILITE, Continuum Company, Santa

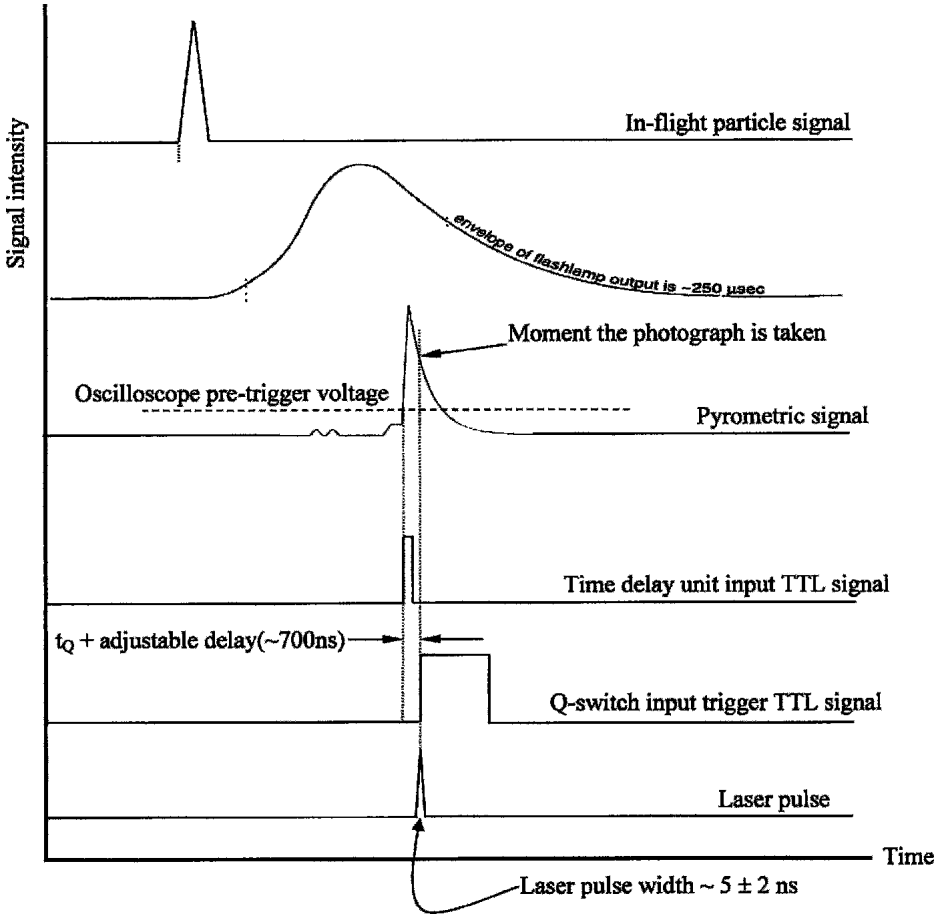

Fig. 3 Sequence of events for triggering the laser.

Clara, CA) were used. Ambient light was low enough that the camera image was recorded by illumination from the laser alone. The laser pulse duration was three orders of magnitude shorter than typical droplet spreading times (~2 μs). The laser pulse was emitted once the Q-switch (a crystal, quarter-wave plate and a horizontal polarizer, placed in the laser cavity between its end mirrors) was triggered. The Nd:YAG medium of the laser was excited by pumping it with a flash lamp.

To maximize image contrast, particles were illuminated from the front and photographed from behind through the glass substrate so that spreading droplets were silhouetted against a brightly lit background (Fig. 1). An 80% neutral density filter was placed in front of the microscope to attenuate the intensity of the laser beam. A ground glass plate was placed in front of the exit of the laser beam to diffuse its light and increase the illuminated area.

When a molten molybdenum droplet emerged from the last of the three holes (Fig. 1), its thermal radiation was detected by an optical detector. This signal was used to trigger the flash lamp of the Nd:YAG laser, a process that required a minimum of 150 μs, before triggering the Q-switch. Because the last shielding plate was placed more than 20 mm from the substrate, there was enough time (130-160 μs, assuming droplet velocities of 120-150 m/s) before the droplet landed. When the droplet impacted on the glass substrate, it produced a sudden rise in the detected signal (point *f* in Fig. 2b). When the signal exceeded a certain predetermined threshold, the digital oscilloscope sent a pulse to trigger a delay generator (model 9650A. Princeton Applied Research, Gamble Technologies Limited, Mississauga, ON). After a predetermined time delay, the Q-switch was activated, sending a laser pulse to illuminate the impacting droplet and take a photograph. The threshold level was adjusted at a level just high enough so in-flight particles did not trigger the delay generator. The response times of the oscilloscope (600 ns), time delay generator (~40 ns), and Q-switch (~60 ns) gave a total delay of 700 ns, which was the minimum time before a photograph could be taken. By varying the time delay different stages of droplet impact were observed. Figure 3 shows a diagram of the sequence of events required to trigger the laser.

Images taken by the CCD camera were digitized by a frame grabber and recorded on a PC. Because we did not photograph the droplet directly, but rather its reflection in a mirror that was inclined to the substrate, images were rotated and foreshortened along one axis. To measure the degree of foreshortening, a plate with an 800-μm circular pinhole was placed on the substrate and photographed. Images were determined to be rotated 60° CCW and foreshortened 70% along one axis. Splat diameters could be measured from photographs with a precision of ±5%.

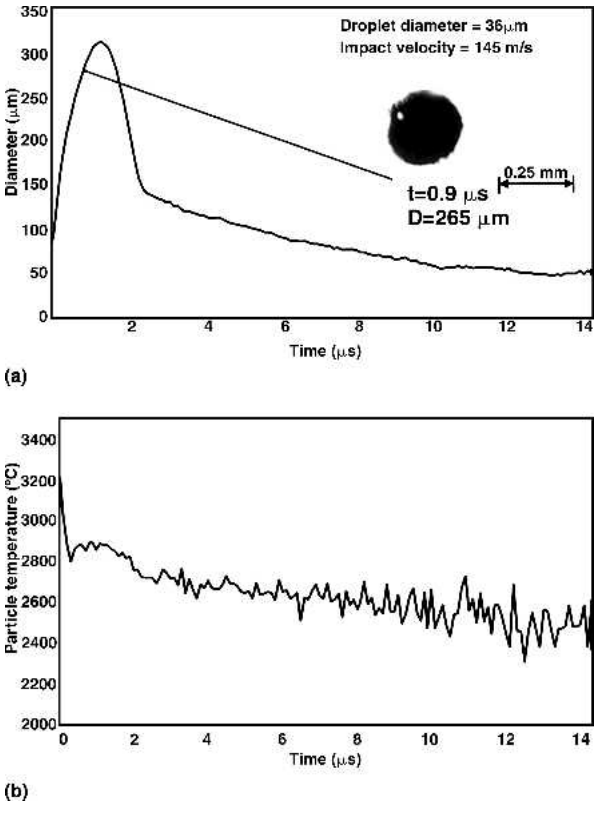

Fig. 4 Variation of (a) diameter and (b) temperature during impact of a 36 μm molybdenum droplet impacting with 145 m/s impact velocity on a glass surface. Inset shows a photograph of the droplet at t = 0.9 μs after impact.

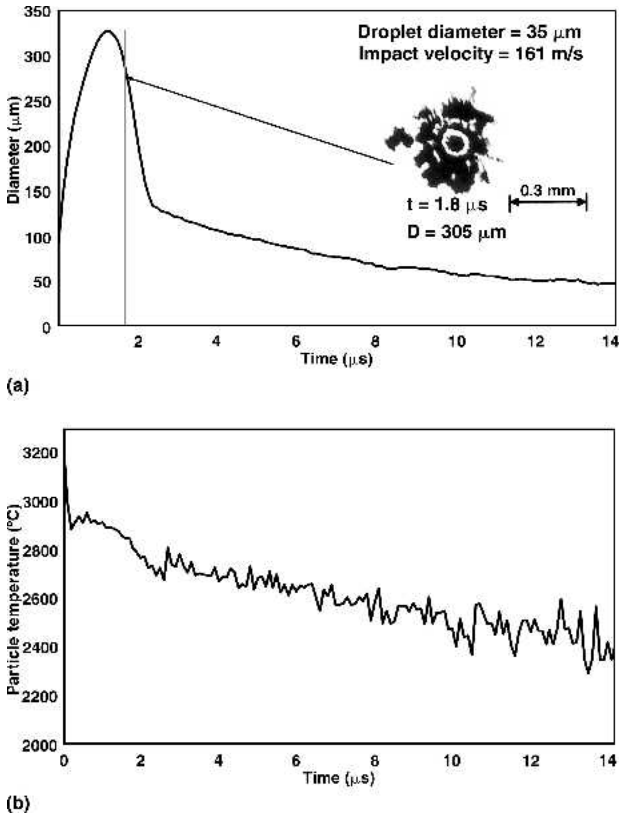

Fig. 5 Variation of (a) diameter and (b) temperature during impact of a 35 μm molybdenum droplet impacting with 161 m/s impact velocity on a glass surface. Inset shows a photograph of the droplet at t = 1.8 μs after impact.

3. Results and Discussion

Figure 4 shows a typical set of results recorded during impact of a 36 μm molybdenum droplet impacting with 145 m/s velocity on a glass substrate initially at room temperature. The photodetector signal was converted into an equivalent droplet diameter measurement, assuming that the impacting droplet was a disk with an emissivity of 0.6. Figure 4(a) shows the variation of equivalent droplet diameter with time (t), measured from the instant that the droplet landed on the surface. The droplet diameter increased until it reached a maximum in approximately 1 μs and then dropped, initially very rapidly and subsequently more slowly. A photograph of the impacting droplet, taken 0.9 μs after impact, is shown in the inset of Fig. 4(a). The droplet was lit from behind, so black areas represent its silhouette. The droplet was still intact and fairly circular at this time. The calculated equivalent diameter at this instant was 265 μm, which agreed reasonably well with the diameter observed in the photograph.

Figure 4(b) shows the corresponding temperature variation of the particle during impact. The temperature was initially 3238 °C, well above the melting point of molybdenum (2617 °C). There was a rapid drop in droplet temperature upon impact followed by a period of relatively constant temperature, which corresponded to the width of the peak from the photodetector. The temperature signal then declined slowly while showing large noise fluctuations.

Figure 5(a) shows a similar set of data for impact of a 35 μm diameter droplet landing with 161 m/s velocity. A photograph of the droplet was taken 1.8 μs after impact, shortly after the peak of the equivalent diameter curve. The calculated diameter was 305 μm, but the photograph showed that the droplet was no longer intact. A small amount of material remained at the center of the droplet, attached to the substrate at the point of impact of the droplet. The film of liquid around it had detached from the center and had several perforations. The temperature recorded by the pyrometer (Fig. 5b) was still relatively constant at approximately 2850 °C.

Droplets disintegrated almost completely toward the end of impact. Figure 6 shows a photograph taken 2.6 μs after impact of a 30-μm droplet with a velocity of 181 m/s. A central core of material remained on the substrate, but there was only a small amount of debris left in the field of view. The calculated equivalent diameter of 116 μm had little physical meaning because it was based on the assumption of an intact droplet. The rate at which the equivalent diameter was decreasing also became much slower after this time, and the temperature measurement showed larger fluctuations as a result of the optical sensors viewing the substrate rather than the droplet.

To determine how the droplet shape changes with time during impact, a number of photographs were taken with varying delays. Figure 7 shows photographs of molten molybdenum droplets during different stages of impact on a glass substrate at

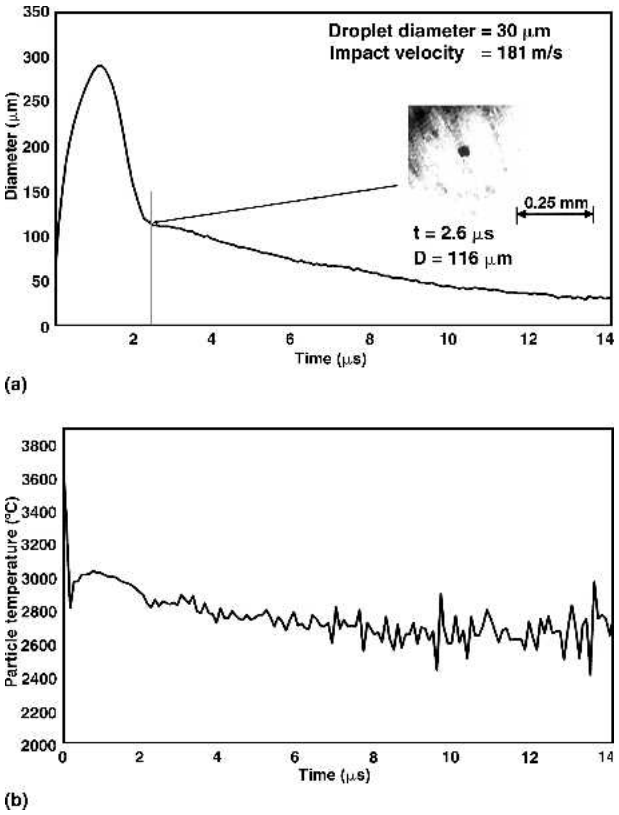

Fig. 6 Variation of (a) diameter and (b) temperature during impact of a 30 μm molybdenum droplet impacting with 181 m/s impact velocity on a glass surface. Inset shows a photograph of the droplet at $t = 2.6$ μs after impact.

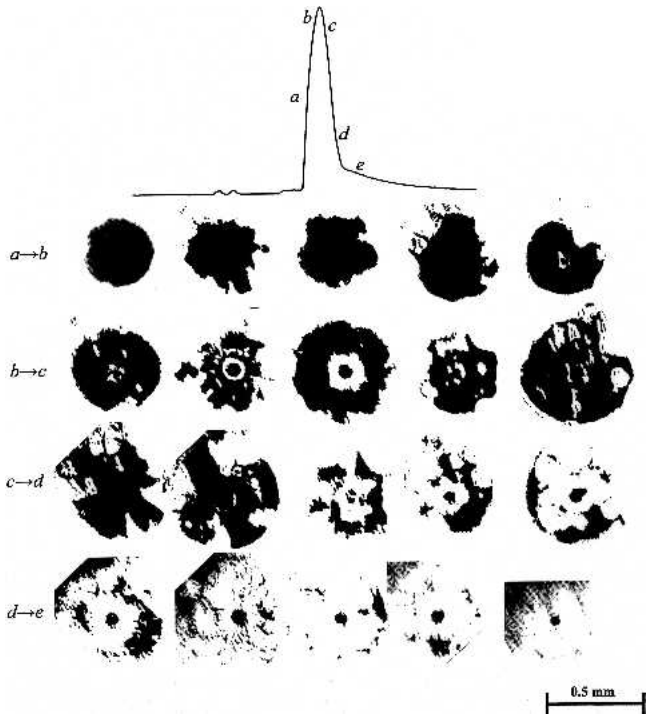

Fig. 7 Photographs of impacting droplets. Each row shows five photographs at approximately the same time after impact. The corresponding time on the optical detector signal is indicated by labels *a* to *e*.

room temperature. Initial droplet diameters in these photographs ranged from 30 to 50 μm, impact velocity from 120 to 160 m/s, and initial droplet temperature from 3200 to 3700 °C. These initial impact conditions correspond to Weber numbers (We) ranging from 2400 to 4500 and Reynolds numbers (Re) ranging from 11,000 to 27,000. Droplet splashing caused by fluid instabilities has been identified (Ref 15) with values of the splash parameter, defined as $K = \mathrm{We}^{0.5}\mathrm{Re}^{0.25}$, in excess of 58. In these experiments K was always greater than 500, so that splashing was expected. Each row of photographs in Fig. 7 shows five droplet images taken at approximately the same time after impact. The moment of impact was defined as the instant the signal from the optical detector showed a sudden increase. Labels *a-e* on the typical optical detector signal shown in Fig. 7 indicate four different time intervals in which pictures were taken.

In the earliest interval *a-b* (ranging from 0.7 to 1 μs after impact), droplets spread very rapidly, creating a liquid film estimated to be approximately 0.5 μm thick, assuming that the splats were disks with the same volume as the original spherical droplets. The film was roughly circular and mostly intact. The thin film became unstable as it spread further and began to break up, producing a peak in the optical signal (interval *b* to *c,* which was from 1 to 1.3 μs after impact). A small portion of the droplet adhered to the surface at the point of impact while the remaining film ruptured.

In the interval *c* to *d* (1.3-1.6 μs after impact) the optical signal showed a sharp decrease. This is partly the result of cooling of the droplet in contact with the substrate. However, photographs showed that the droplet surface area seen by the detector decreased rapidly as portions of the droplet recoiled because of the surface tension of the molten metal. Indeed, it has been shown that during this time period, no significant amount of material flew out of the field of view of the detectors (Ref 12, 13). Consequently, the decrease of the droplet surface area was mostly attributed to the recoil of the droplet fragments. In the final stages (*d* to *e*, 1.6-2.0 μs after impact), molybdenum portions flew off the surface, and the detector signal decreased slowly. Photographs showed that there was almost no metal remaining in the image, except for the small spot attached to the point where the droplet first landed surrounded by a ring of debris. The central spot was approximately 30 μm in diameter, approximately the same as that of the original spherical droplet.

All of the photographs shown so far were taken using a 5 ns laser pulse as a light source to eliminate blurring caused by movement. A few additional pictures, shown in Fig. 8, were taken using a much longer-duration light source, a strobe that provided an 8 μs flash (model MVS 7000, EG&G Corp., Salem, MA). To increase image contrast, a photograph of the substrate before droplet deposition was subtracted from the picture of the impacting droplet using image analysis software. The resulting picture is integrated over the entire flash duration. The relative darkness of any point in the image corresponds to the time it was covered by the droplet. The frames on the right show photographs of material still remaining on the substrate after droplet impact.

Figure 8(a) was taken with the flash triggered at the instant of

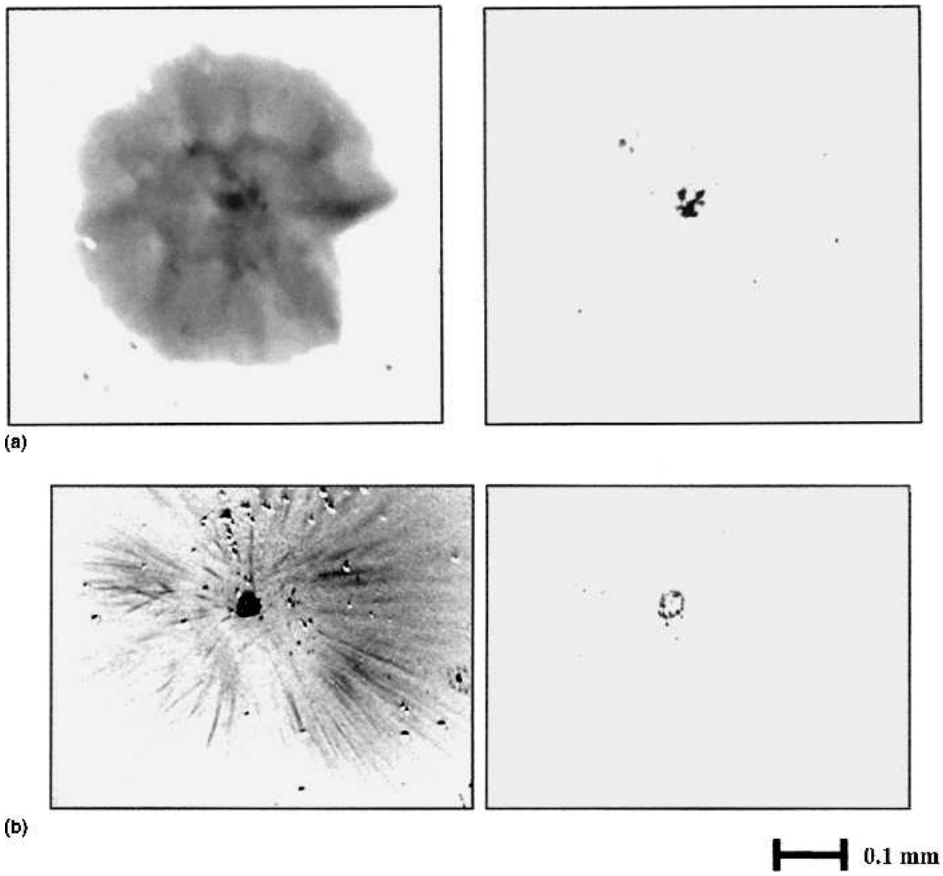

Fig. 8 Photographs of impacting droplet taken with an 8 μs flash triggered (a) at the instant of impact and (b) 4 μs after impact. The frames on the right show the material remaining on the surface after impact.

impact and shows the next 8 μs of impact. The extent to which the droplet spread while still intact can be seen clearly. The droplet broke up after impact, leaving only a small amount of material on the surface. In Fig. 8(b) the flash was triggered 4 μs after impact and shows the subsequent 8 μs. It integrates over times significantly later than the photographs in Fig. 7 taken at $t < 2$ μs. Radial streaks show fragments of the drop flying away from the point of impact. This technique allows us to capture particles that may have been too small to see with a 5 ns exposure.

4. Conclusions

A technique was developed to photograph the impact of molten molybdenum droplets (~40 μm in diameter) impinging with high velocities (~140 m/s) on a glass substrate initially at room temperature. Two light sources were used, one a 5 ns pulsed laser and the other an 8 μs strobe. The short duration laser pulse froze all motion, whereas the longer illumination produced an image that integrated over the entire impact process and showed small, fast-moving particles as streaks. Photographs showed that droplets first expanded rapidly (in about 1 μs) to form a thin film, less than 0.5 μm in thickness. This film was unstable and ruptured at several points. A small portion of the droplet remained attached to the surface at the point of impact while the remaining mass fragmented and flew off the surface. The entire impact lasted approximately 2 μs. An optical detector recording thermal radiation from the impacting droplet gave a signal that increased as the droplet spread out, reached a maximum when the liquid film began to rupture, and then decreased as portions of the droplet recoiled under surface tension and flew out of view of the photodetector.

References

1. N. Sakakibara, H. Tsukuda, and A. Notomi, The Splat Morphology of Plasma-Sprayed Particle and the Relation to Coating Property, *Thermal Spray: Surface Engineering via Applied Research,* C.C. Berndt, Ed., May 8-11, 2000 (Montréal, Québec, Canada), ASM International, 2000, p 753-758
2. V. Pershin, M. Lufitah, S. Chandra, and J. Mostaghimi, Effect of Substrate Temperature on Adhesion Strength of Plasma-Sprayed Nickel Coatings, *J. Thermal Spray Technol.,* Vol 12, 2003, p 370-376
3. L. Bianchi, F. Blein, P. Lucchese, M. Vardelle, A. Vardelle, and P. Fuchais, Effect of Particle Velocity and Substrate Temperature on Alumina and Zirconia Splat Formation, *Thermal Spray Industrial Applications,* C.C. Berndt and S. Sampath, Ed., June 20-24, 1994 (Boston, MA), ASM International, 1994, p 569-574
4. J. Pech, B. Hannoyer, A. Denoirjean, and P. Fauchais, Influence of Substrate Preheating Monitoring on Alumina Splat Formation in DC Plasma Process, *Thermal Spray: Surface Engineering via Applied Research,* C.C. Berndt, Ed., May 8-11, 2000 (Montréal, Québec, Canada), ASM International, 2000, p 759-765

5. C.J. Li, J.L. Li, W.B. Wang, A. Ohmori, and K. Tani, Effect of Particle Substrate Materials Combinations on Morphology of Plasma-Sprayed Splats, *Thermal Spray: Meeting the Challenges of the 21st Century,* C. Coddet, Ed., May 25-29, 1998 (Nice, France), ASM International, 1998, p 481-487
6. C.J. Li, J.L. Li, and W.B. Wang, The Effect of Substrate Preheating and Surface Organic Covering on Splat Formation, *Thermal Spray: Meeting the Challenges of the 21st Century,* C. Coddet, Ed., May 25-29, 1998 (Nice, France), ASM International, 1998, p 473-480
7. X. Jiang, Y. Wan, H. Hermann, and S. Sampath, Role of Condensates and Adsorbates on Substrate Surface on Fragmentation of Impinging Molten Droplets during Thermal Spray, *Thin Solid Films,* Vol 385, 2001, p 132-141
8. M. Fukumoto, S. Kato, and I. Okane, Splat Behavior of Plasma-Sprayed Particles on Flat Substrate Surface, *Thermal Spraying: Current Status and Future Trends,* A. Ohmori, Ed., May 22-26, 1995 (Kobe, Japan), High Temperature Society of Japan, 1995, p 353-358
9. M. Pasandideh-Fard, V. Pershin, S. Chandra, and J. Mostaghimi, Splat Shapes in a Thermal Spray Coating Process: Simulations and Experiments, *J. Thermal Spray Technol.,* Vol 11, 2002, p 206-217
10. C. Moreau, P. Cielo, M. Lamontagne, S. Dallaire, and M. Vardelle, Impacting Particle Temperature Monitoring during Plasma Spray Deposition, *Meas. Sci. Technol.,* Vol 1, 1990, p 807-814
11. M. Vardelle, A. Vardelle, P. Fauchais, and C. Moreau, Pyrometer System for Monitoring the Particle Impact on a Substrate during a Plasma Spray Process, *Meas. Sci. Technol.,* Vol 5, 1994, p 205-212
12. P. Gougeon and C. Moreau, Simultaneous Independent Measurement of Splat Diameter and Cooling Time during Impact on a Substrate of Plasma-Sprayed Molybdenum Particles, *J. Thermal Spray Technol.,* Vol 10 (No. 1), 2001, p 76-82
13. C. Moreau, J.-F. Bisson, R.S. Lima, and B.R. Marple, Diagnostics for Advanced Materials Processing by Plasma Spraying, *Pure and Applied Chem.,* Vol 77 (No. 2), 2005, p 443-463
14. P. Gougeon, C. Moreau, V. Lacasse, M. Lamontagne, I. Powell, and A. Bewsher, *Advanced Processing Techniques: Particulate Materials,* Vol 6, Metal Powder Industries Federation, Princeton, NJ, 1994, p 199-210
15. P. Fauchais, Understanding Plasma Spraying, *J. Phys. D Appl. Phys*., Vol 37, 2004, p R86-R108